

M. CIEŚLA<sup>\*,#</sup>, M. MAŃKA<sup>\*</sup>, F. BINCZYK<sup>\*</sup>, P. GRADOŃ<sup>\*</sup>**CREEP BEHAVIOUR OF MODIFIED MAR-247 SUPERALLOY**

The paper presents the results of analysis of creep behaviour in short term creep tests of cast MAR-247 nickel-based superalloy samples made using various modification techniques and heat treatment. The accelerated creep tests were performed under temperature of 982 °C and the axial stresses of  $\sigma = 150$  MPa (variant I) and 200 MPa (variant II). The creep behaviour was analysed based on: creep durability (creep rupture life), steady-state creep rate and morphological parameters of macro- and microstructure. It was observed that the grain size determines the creep durability in case of test conditions used in variant I, durability of coarse-grained samples was significantly higher.

*Keywords:* nickel superalloys, creep, macrostructure, microstructure

**1. Introduction**

Heat resistant nickel based alloys are main materials used in manufacturing of the responsible parts of aircraft engine turbines [1-5]. These parts, like combustion chambers and turbine blades, are often subjected to very high temperature. In case of turbine blades the work temperature, depending on blade type, mounting type and heat dissipation, is in the range from 700 to 1100 °C [4,5]. The adverse effects of high temperature result from i.a. intensification of corrosion processes, changes of material microstructure and decrease of mechanical properties. Simultaneously, high temperature create favourable conditions for permanent deformations, especially during creep processes [4,5,8].

The efficient application of heat resistant nickel superalloys used in turbine blades of aircraft engines requires an understanding of the creep mechanisms dominant under certain operating conditions [10]. Particularly important is to assess the durability of material in the short term creep test, as it provides information about the destruction processes under extreme operating conditions. These type of test are used by engine manufactures (such as Pratt&Whitney Rzeszów) as one of the main selection criterions for nickel-based superalloys. Short term creep tests are also used in assessment of effectiveness of high temperature protective coatings [4-7].

Various critical aircraft engine parts are manufactured from alloys such as: IN-100, IN-738, IN-713C, RENE-77, RENE-80, MAR-257. These are precipitation-hardened alloys which develop specific macrostructure during solidification consisting of equiaxial and columnar grains and frozen crystals zone. Such structure can be the cause of formation and propagation of cracks and thus cause serious engine failures [8,9]. In case of the turbine blades, the good understanding of cracking in creep conditions allows for proper selection of materials, modification and heat treatment

procedures and thus obtain optimal material characteristics such as microstructure and mechanical properties. Some of the methods of structure refinement are the surface [11-13], volume [14-16] and combined surface and volume modification techniques [17,18]. This processes allow for obtaining grains of various dimensions, orientation and distribution. The ability to influence the grain characteristics allows for control of mechanical properties.

The optimal grain size for aircraft engine parts made of nickel superalloys depends on the work conditions. Under typical workload of aircraft turbine (Fig. 1) the steady state creep rate  $V_s$  (1) decrease with the increase of grain size [7,8] while yield point and tensile strength usually decrease [16,19]. Grain boundaries absorb the dislocations which results in reduction of deformation strengthening. Additionally the mechanism of grain boundary slide adversely affects the durability in this condition [8].

$$V_s = \frac{B\sigma\delta}{kT} \frac{\Omega}{d^3} \frac{D_{GB}}{d^3} \quad (1)$$

where: B – material constant,  $\sigma$  – stress,  $\delta$  – effective grain boundary thickness,  $\Omega$  – atomic volume,  $D_{GB}$  – grain boundary diffusion coefficient, k – Boltzmann constant, T – absolute temperature, d- grain diameter.

This paper presents the analysis of creep behaviour of castings made of nickel superalloy MAR-247 obtained using various modification techniques and subjected to heat treatment. The accelerated creep tests were carried out under the temperature of 982 °C and axial stress of  $\sigma = 150$  and 200 MPa. The creep behaviour was analysed using obtained values of creep rupture life, steady-state creep rate and macrostructure characteristics. The dominant creep mechanisms were identified by comparison with data obtained for alloy of similar chemical composition (Fig. 1) [8-10].

\* SILESIA UNIVERSITY OF TECHNOLOGY, 8 KRASIŃSKIEGO STR., 40-018 KATOWICE, POLAND

# Corresponding author: marek.ciesla@polsl.pl

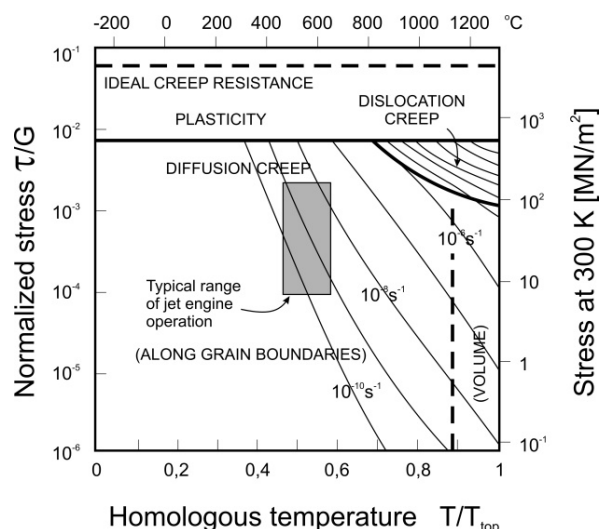


Fig. 1. Map of deformation mechanisms in MAR-M-200 alloy, grain size 100  $\mu\text{m}$  [8]

## 2. Methods and materials

Castings used in this study were made of MAR-247 scrap of chemical composition presented in TABLE 1 and were produced in two following experiments:

- Experiment 1 – cast to modifying (“blue”) mould with modifying (“blue”) filter.
- Experiment 2 – cast to non-modifying (“white”) mould with modifying (“blue”) filter.

TABLE 1  
Chemical composition of MAR-247 nickel superalloy

Material	Content, wt. %					
	Cr	Mo	Co	Ti	Al	Nb
MAR-247	9.05	0.78	9.48	1.12	5.52	0.12
	W	C	Hf	Ta	Si	Zr
	11.2	0.112	1.18	3.78	0.08	0.04
Ni – 57,54						

Melting and casting was carried out in Leybold-Heraeus JS5/III vacuum induction furnace in  $\text{Al}_2\text{O}_3$  crucible using ceramic moulds made by the lost wax casting technology. Modification mixture contained cobalt aluminate  $\text{CoAl}_2\text{O}_4$  which gave it characteristically blue colour, hence the naming “blue” and “white”. Moulds were prepared according to procedures of combined volume and surface modification with double filtration [16-18].

In the next phase of the study castings were subjected to heat treatment typical for this type of alloy – solutionizing at 1185 °C for 2 h and aging at 870 °C for 20 h. Standard creep test samples were manufactured using obtained material. Creep tests were performed in Walter-Bai AG LFMZ-30kN using various parameters (TABLE 2) similar to workload of turbine blades in aircraft turbojet engines and corresponding to acceptance report parameters of turbine manufacturers.

In order to determine the factors influencing the creep processes and creep durability (characterised by creep rupture life) of studied materials the analysis of macro- and microstructure were performed.

Macrostructure analysis was carried out using the specimens made from cross-sections of the creep test samples by etching with Marble solution. The grain characteristics were determined using Met-Ilo image analysis software.

Microstructure analysis was performed on metallographic section specimens using Hitachi S-4200 scanning electron microscope (SEM) and on thin film specimens using Hitachi HD-2300 scanning transmission electron microscope (STEM). Chemical composition analysis was carried out using energy-dispersive X-ray spectroscopy (EDX) and phase composition was identified by electron nanodiffraction.

TABLE 2  
Characteristics of MAR-247 samples characteristics and creep test parameters

Sample No	Microstructure characteristic		Creep condition test	
1	fine grain		variant I	T = 982 °C σ = 150 MPa
2	coarse grain			
3	after HT	fine grain		
4		coarse grain		
5	fine grain		variant II	T = 982 °C σ = 200 MPa
6	coarse grain			

## 3. Results and discussion

Creep curves for superalloy MAR-247 plotted using data obtained during the experiments are presented on Fig. 2 and Fig. 3. TABLE 3 presents the collated results of microstructural analysis and creep tests.

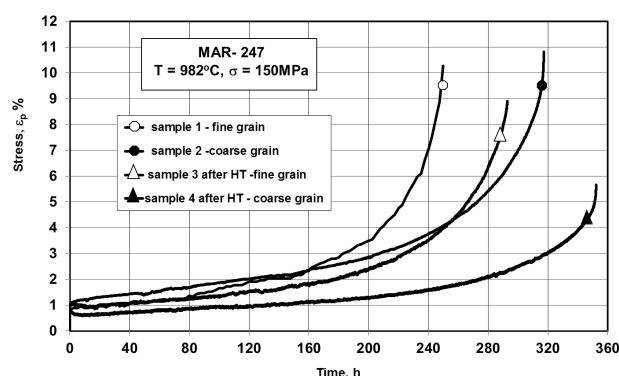


Fig. 2 Creep curves of MAR-247 in as-cast state (sample 1, 2) and after heat treatment (sample 3, 4) – variant I of creep test

In the first variant creep tests (TABLE 2) the creep durability (creep rupture life) both in as-cast state and after the heat treatment was significantly affected by grain size. The longer creep rupture life was observed for castings with coarse grain, compared to fine grained structures the increase was respectively 27 % and 20 %. Analysis of deformation mechanism maps (Fig. 1) and literature references enable to assume that, the creep deformation of samples 1 to 4 was mainly influenced by diffusion creep [8-10]. The durability of material after the heat treatment was further increased by several percent (TABLE 3).

In the second variant of creep tests the higher axial stress  $\sigma$  created the conditions in which the durability was independent of grain size (TABLE 3). Only few hour differences in creep rupture life were observed between fine and coarse grained samples (samples 5 and 6).

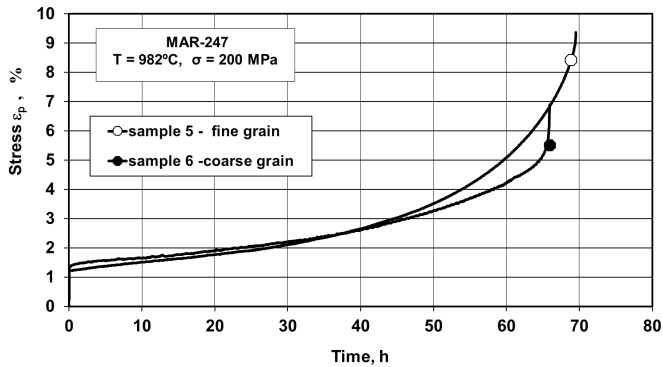


Fig. 3 Creep curves of MAR-247 in as-cast state (sample 5, 6) – variant II of creep test

In the studied materials the primary carbides were of “script” morphology and gathered mainly on grain boundaries. As shown in TABLE 3, the durability of materials in the first variant creep tests was strongly influenced by the area fraction of carbides  $A_A$  per number of grains  $N$  or the  $A_A/N$  parameter. With the increase of this parameter the creep rupture life increased and the steady-state creep rate decreased (TABLE 3). In the second variant of creep test the parameter  $A_A/N$  was less influential which indicates at the reduced role of grain boundary strengthening.

Microanalysis of chemical composition of MAR-247 samples after the creep tests revealed the thin layer of oxides composed of Cr, Al and Ti on the surface. In subsurface areas of the samples the  $\gamma'$  phase was undergoing dissolution as a result of depletion of oxidizing elements (Figs. 4). In the subsequent creep stages in this zone the cracking processes

were initiated (Figs. 4, 5). The cracks then propagated along the grain boundaries and finally caused rupture of the sample. Microstructure analysis of samples after the creep test revealed changes of the morphology of  $\gamma'$  phase – so called rafting (Fig. 6) [19,20].

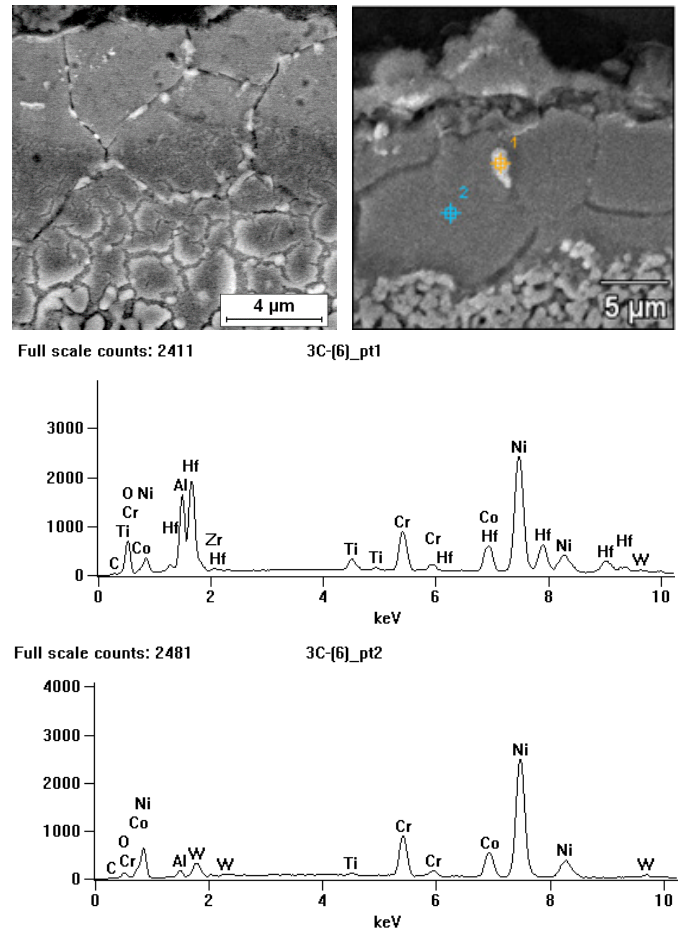


Fig 4. SEM images and EDX analysis showing degradation of surface areas in sample no 5

TABLE 3

Morphological parameters and creep characteristics of tested samples

Sample No	Structure	Number of grain $N$	Mean plane section area of grain $A$ [mm <sup>2</sup> ]	Area fraction of carbides $A_A$ [%]	Area fraction of carbides per grain $A_A/N$ [%]	Steady state creep rate $V_s$ [s <sup>-1</sup> ]	Creep rupture life $t_z$ [h]
1	fine grain	45	0.57	2.12	0.047	$2.5 \times 10^{-8}$	250
2	coarse grain	7	3.55	1.45	0.210	$2.2 \times 10^{-8}$	317
3	fine grain after HT	24	1.09	1.95	0.08	$1.66 \times 10^{-8}$	293
4	coarse grain after HT	10	2.68	1.91	0.19	$1.06 \times 10^{-8}$	352
5	fine grain	29	0.90	2.51	0.087	$2.34 \times 10^{-5}$	69
6	coarse grain	7	3.81	2.29	0.327	$2.58 \times 10^{-5}$	65



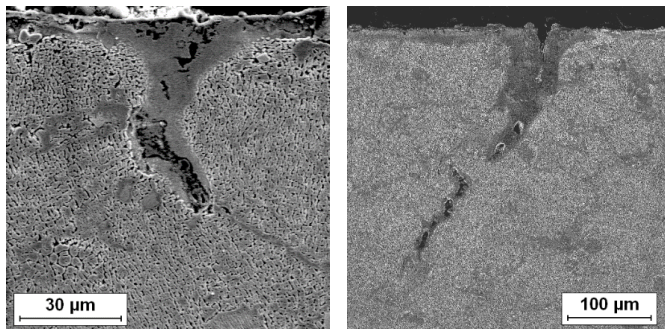


Fig. 5. SEM images of cracks in sample no 5

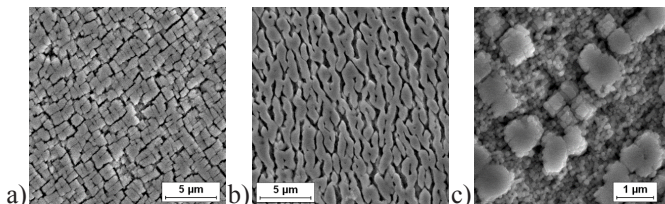


Fig. 6. SEM images of changes in morphology of  $\gamma'$  phase: a) as-cast, b) after creep test (rafting), c) after heat treatment

Particular type of degradation in subsurface areas was observed in samples which undergone the second creep test variant. The oxidation of the matrix grain boundaries leading to formation of many, fine particles of oxide phase containing Hf (Fig. 4).

Complex oxides, rich in Hf, are characterised by high values of Pilling-Bedworth coefficient  $R_B$  (about 2.6 [21]). This may indicate that the presence of such oxides on grain boundaries caused more rapid cracking.

Microanalysis of thin foils using EDX and nanodiffraction revealed the presence of fine  $M_6C$  carbide participates. The following assumption was formulated: when  $(Cr \text{ at.}\%)/((Cr+Mo+0.7W) \text{ at.}\%) > 0.82$  the Cr rich  $M_{23}C_6$  carbides evolve, in case of values  $< 0.72$  the W and Mo rich  $M_6C$  are formed. This fine carbide particles were absent from samples in the cast state, before the creep tests. Identified  $M_6C$  carbides may play an important role in the process of deformation under creep conditions by strengthening the alloy matrix.

#### 4. Conclusions

The variant I creep tests (TABLE 2) showed that the creep durability (creep rupture life) of coarse-grained samples were higher (Fig. 2). The application of heat treatment significantly raised the durability in respect to as-cast samples.

Creep durability of MAR-247 determined in variant II creep tests using higher stress values (TABLE 2) was significantly lower than in variant I tests. At the same time in the variant II tests show that under these conditions the grain size have no influence on time to rupture (Fig. 3).

Microscopic observations showed that the heat treatment procedure lead to considerable fragmentation of  $\gamma'$  phase (Fig. 6) which probably is the main cause of higher durability of this samples.

Microstructure analysis of variant II samples showed change of morphology of  $\gamma'$  phase precipitates, the so called rafting phenomenon (Fig. 6).

Analysis of obtained results showed a relationship between creep durability and fraction of carbides  $A_A$  per number of grains  $N$  (TABLE 3) in variant I samples.

#### Acknowledgement

Financial support of Structural Funds in the Operational Programme - Innovative Economy (IE OP) financed from the European Regional Development Fund - Project "Modern material technologies in aerospace industry", No. POIG.01.01.02-00-015/08-00 is gratefully acknowledged.

#### REFERENCES

- [1] C.T. Sim, N.S. Stolaf, W.C. Hagel, *Superalloys II*, Wiley, New York 1987.
- [2] Z. Dzygało, M. Łyżwiński, J. Otyś, S. Szczeciński, R. Wiatrek: *Zespoły wirnikowe silników turbinowych*, WKŁ, Warszawa 1982.
- [3] A.K. Koul, V.R. Parameswaran, J.P. Immarrigeon., W. Wallace, *Advances in High Temperature Structural Materials and Protective Coatings*, National Research Council of Canada, Ottawa 1994.
- [4] J. Sieniawski, *Kryteria i sposoby oceny materiałów na elementy lotniczych silników turbinowych*, Oficyna Wyd. Politechniki Rzeszowskiej, Rzeszów 1995.
- [5] M.J. Donachie, S.J. Donachie, *Superalloys A Technical Guide*, ASM International, Materials Park 2002.
- [6] Y. Tamarin, *Protective Coatings for Turbine Blades*, ASM International, Materials Park 2002.
- [7] A. Strang, *High Temperature Properties of Coated Superalloys*, in: *Behaviour of High Temperature Alloys in Aggressive Environments*, Metals Society, London (1980).
- [8] J. Wyrzykowski, E. Pleszakow, J. Sieniawski, *Odształcanie i pękanie metali*, WNT, Warszawa 1999.
- [9] Z.L. Kowalewski, *Zjawisko pękania metali*, WIPPT PAN, Warszawa 2005.
- [10] Frost H.J., Ashby M.F., *Deformation-Mechanism Maps - The plasticity and creep of metals and ceramics*, Pergamon Press, Oxford 1982.
- [11] M. Zielińska, J. Sieniawski, M. Wierzbńska, *Arch. Metal. Mater.* **53**, 887 (2008).
- [12] F. Binczyk, J. Ślężiona, *Arch. Foundry Eng.* **10**, 195 (2010).
- [13] M. Zielińska, J. Sieniawski, M. Poręba, *Arch. Mater. Sci. Eng.* **28**, 10 (2007).
- [14] F. Binczyk, J. Ślężiona, *Arch. Foundry Eng.* **10**, 9 (2010).
- [15] F. Binczyk, J. Ślężiona, P. Gradoń, *Composites* **11**, 49 (2011).
- [16] M. Cieśla, F. Binczyk, M. Mańka, *Arch. Foundry Eng.* **12**, 17 (2012).
- [17] F. Binczyk, J. Ślężiona, P. Gradoń, *Arch. Foundry Eng.* **11**, 29 (2011).
- [18] F. Binczyk, P. Gradoń, M. Mańka, *Arch. Foundry Eng.* **12**, 5 (2012).
- [19] F.R.N. Nabarro, C.M. Cress, P. Kotschy, *Acta Mater.* **44**, 3189 (1996).
- [20] A. Epishin, T. Link, *Philos. Mag.* **84**, 1979 (2004).
- [21] M. Blicharski, *Wstęp do Inżynierii Materiałowej*, WNT, Warszawa 2001.